**Morteza Haghshenas[1,*], Hamid Falaghi[1],**

J. Electrical Systems 12-1 (2016): 85-101

**Regular paper**

Journal of Electrical Systems

# Environmental/Economic Operation Management of a Renewable Microgrid with Wind/PV/FC/MT and Battery Energy Storage Based on MSFLA

Microgrids (MGs) are local grids consisting of Distributed generators, energy storage systems and dispersed loads which may operate in both grid-connected and islanded modes. This paper aims to optimize the operation of a typical grid-connected MG which comprises a variety of DGs and storage devices in order to minimize both total operation cost and environmental impacts resulted from supplying local demands. Furthermore we will try to achieve an intelligent schedule to charge and discharge storage devices that provides the opportunity to benefit from market price fluctuations. The presented optimization framework is based on multiobjective modified shuffled frog leaping algorithm (MSFLA). To solve environmental/economic operation management (EEOM) problem using MSFLA, a new frog leaping rule, associated with a new strategy for frog distribution into memeplexes, is proposed to improve the local exploration and performance of the ordinary shuffled frog leaping algorithm. The proposed method is examined and tested on a grid-connected MG including fuel cell, wind turbine, photovoltaic, gas-fired microturbine, and battery energy storage devices. The simulation results for three scenarios involving the economic operation management of MG, environmental operation management of MG, and environmental/economic operation management of MG are presented separately. The obtained results compared with results of well-known methods reported in the literature and prove the efficiency of the proposed approach to solve the both single objective and multiobjective operation management of the MG.

Keywords: Microgrid, Renewable Energy Sources, Environmental/Economic Operation Management (EEOM), Modified shuffled frog leaping algorithm (MSFLA).

Article history: Received 16 November 2015, Accepted 4 February 2016

## 1. Introduction

In recent years, high utilization of renewable energy sources (RESs) in the form of distributed generations (DGs) has experienced rapid growth especially in the voltage level of distribution networks. Along with the potential capability to provide reliable, efficient and secure electricity, Distributed Energy Resources (DERs) offer consumers and electric utilities many economical and environmental benefits. However, from the operation management point of view, the high penetration of renewable DGs can bring some unwanted challenges which a significant part is covered in the form of Microgrid (MG). MG is a local grid consisting of DGs, energy storage systems and dispersed loads which may operate in both grid-connected and islanded modes [1]. MGs which are referred to as

* Corresponding author: Morteza Haghshenas, Department of Electrical Power Engineering, Faculty of Electrical and Computer Engineering, University of Birjand, Birjand, Iran. (Haghshenas.Research@gmail.com)
[1] Department of Electrical Power Engineering, Faculty of Electrical and Computer Engineering, University of Birjand, Birjand, Iran. (Haghshenas.Research@gmail.com), (Falaghi@birjand.ac.ir)

building blocks of the smart grids require a central management unit which monitors system status and makes the necessary decisions in order to optimize MG operation aligned with desired objectives while considering system constraints and regulatory rules [2–3]. In this regard, in recent years, several researches have been implemented to investigate the MG operation Management under different loading with different targets.

Minimization of the operation cost or in other words meeting the load demand in the most economical way is an important objective which has been seeking by researchers as [4–14] provide methods in order to reduce the operation cost of a MG containing battery storage. In [4], proposed a centralized MG control and assessed the optimal operation of the MG by optimizing both the active power of the DG units and power exchange with the upstream distribution network. A linear programming algorithm is proposed in [5] to optimize MG operation cost and battery charge states. In [6] a smart energy management system based on the matrix real coded genetic algorithm (GA) to optimize the operation of a MG is presented. In [7], an expert multiobjective adaptive modified particle swarm optimization (PSO) algorithm is proposed and implemented to solve the multi-operation management problem in a typical MG with renewable energy sources. An improved PSO algorithm combined with Monte Carlo simulation is used in [8] to solve the dynamic economic dispatch of a MG. In [9], a heuristic algorithm for the energy management in Islanded MG, which avoids wastage of the existing renewable potential at each time interval, is proposed. In [10], the direct effect of utilization of storage devices on the cost of the MG was investigated through a linear programming technique. Similar work based on participation method was proposed in [11] to solve the unit commitment problem in a renewable MG including storage devices.

On the other hand, in recent years, increased public awareness for the environmental effects of producing electricity has led to devising new strategies in order to reduce emission beside other objectives in optimization scheme. In this regard, minimization of emission, fuel and operation costs are considered in [15–20]. In [15], a framework is presented to optimally schedule the renewable power generators and energy storage in a grid-connected MG reducing the annual cost and emission of MG. In [16], a multi-scenario, multi-objective optimization method of a grid-parallel MG is presented, based on application scenarios' classification, minimizing the annual cost and emission of MG as well as maximizing the utilization of renewable energies. In [17–18], a mesh adaptive direct search algorithm is used to minimize the cost and emission of a grid-connected MG including a fuel cell (FC), a microturbine (MT), a diesel engine generator (DEG), a photovoltaic (PV) system, a wind turbine (WT) and batteries. Multi-objective optimizations of MG operation are transformed into single-objective using a weighted sum method in [15–16],[20]. Similarly, in [17] and [19], emission cost for the units of MG is utilized in the optimization models using emission factor and cost of each emission type.

This paper aims to optimize the operation of a grid-connected MG which comprises a variety of DERs in order to minimize both cost and emission objectives simultaneously. Furthermore we will try to achieve an intelligent schedule to charge and discharge storage devices that provides the opportunity to benefit from market price fluctuations. Also in order to facilitate the process of decision making, MG central controller (MGCC) is provided with a set of optimal solutions to choose a suitable strategy based on desired preferences. The presented optimization framework is based on new modified shuffled frog leaping algorithm (MSFLA). In the procedure proposed in this paper emission factor of DG sources and upstream network are suitably incorporated into the model. Detailed modeling of storage devices' constraints along with utilizing realistic market prices and DG bids has

made the methodology consistent with actual system conditions. The rest of paper is organized as follows. The mathematical EEOM problem formulation is explained in Section 2. Section 3 is dedicated to the details of Distributed generation bids calculation. In Section 4, a brief description of multiobjective optimization and proposed optimization method is provided. The study case is introduced in section 5. Simulation results are presented in Section 6, and finally, the conclusion is given in Section 7.

## 2. Mathematical EEOM Problem formulation

The mathematical model of such a problem can be expressed as follows.

### 2.1. Minimization of Operation Cost

The objective function for total operation cost minimization can be written as

$$C(P) = \sum_{t=1}^{T} Cost(t) = \sum_{t=1}^{T} \left\{ \sum_{i=1}^{N} B_i(P_{gi}(t)) + B_G(t) \;\; P_G(t) \right\} \tag{1}$$

where $P$ is a candidate solution in which $P_{gi}(t)$ and $P_G(t)$ are considered as real output power of $i$th generator and the active power which is bought (sold) from (to) the utility at time $t$ respectively [12]. $T$ is the total number of hours, $N$ is the total number of DG including storage units, $B_i(P_{gi}(t))$ is the bid of the $i$th DG unit as a function of its active power at time $t$, and $B_G(t)$ is the market price of power exchange between the MG and the utility at time $t$ [4].

The cost function (1) can be a nonlinear function because the DG bids are typically either piecewise linear or smooth quadratic functions of $P_{gi}(t)$ [21].

### 2.2. Minimization of Operation Cost

The amount of atmospheric pollutants such as carbon dioxide $CO_2$, sulphur oxide $SO_x$ and nitrogen oxide $NO_x$ caused by fossil-fuelled units either in MG or upstream network is considered in evaluating emission objective as follows

$$E(P) = \sum_{t=1}^{T} \left\{ \sum_{k=1}^{M} \left\{ \sum_{i=1}^{N} P_{gi}(t) \;\; EF_{i,k} + P_G(t) \;\; EF_{G,k}(t) \right\} \right\} \tag{2}$$

where $EF_{i,k}$ and $EF_{G,k}$ represent the emission factor of the $k$th pollutant of the $i$th DG unit and upstream network in g/kWh during hour $t$ respectively. Furthermore $M$ shows the number of considered types of pollutants in the analysis.

### 2.3. Objective Constraints

The problem constraints include both security and limitation constraints which are described bellow.

#### *2.3.1. Power balance constraint*

The total output power of DGs, energy storage devices and main distribution network must cover the total load demand in the MG for each time interval $t$. In this paper the real power loss in the MG is neglected. Accordingly, the power balance constraint can be represented as follows:

$$\sum_{t=1}^{T} P_{gi}(t) + P_G(t) = P_D(t) + P_B(t) \tag{3}$$

In which $P_D(t)$ denotes hourly demand and $P_B(t)$ represents amount of charging/discharging of the battery bank at $t$th hour which is considered positive as it is charging and negative during discharging periods. So during charging periods, demand would be increased as

extra amount of energy is needed in order to charge batteries whereas in discharging time, demand decreases as a result of energy provided by batteries in that hour.

*2.3.2. Generation Capacity Constraint*

For stable operation, the real power output of each unit in the MG, is restricted by minimum and maximum power limits as follows [12], [22]:

$$P_{gi,\min}(t) \le P_{gi}(t) \le P_{gi,\max}(t) \tag{4}$$

where $P_{gi,\min(t)}$ and $P_{gi,\max(t)}$ are the minimum and maximum active powers of the $i$th DG at time $t$. For DGs that use renewable energy sources, upper bound will be their maximum available power at related hour.

*2.3.3. Spinning reserve constraint*

The spinning reserve is necessary to maintain the system reliability, owing to power fluctuations in renewable energy and load fluctuations. To meet the spinning reservation, the following inequality constraint should be satisfied [8], [12]:

$$\sum_{i=1}^{N} P_{gi,\max}(t) + P_{G,\max}(t) \ge P_D(t) + R(t) \tag{5}$$

where $R_t$ is the scheduled spinning reserve at time $t$.

In a MG, the spinning reserve constraint is considered by adding an extra value to the total power demand, which should be supplied by the DG units. It is worth noting that the maximum power capacity (not the operating point) of the power sources is considered in the above equation.

*2.3.4. Battery energy storage constraint*

The battery bank which has been chosen from lead-acid type is utilized to store energy. Considering batteries in optimization plan will result in additional constraints which should be satisfied at all times. State of Charge (SOC) of the battery bank is calculated at each interval using following equation.

$$SOC(t) = SOC(t-1)(1-\delta(t)) + \eta_{charge} \max(0, P_B(t))\Delta t + \frac{1}{\eta_{discharge}} \min(0, P_B(t))\Delta t \tag{6}$$

where SOC($t$) and SOC($t$-1) denote amount of energy stored in the battery at hour $t$ and $t$-$1$ respectively and δ represents self-discharging coefficient. Also $\eta_{charge}/\eta_{discharge}$ is the battery charge/discharge efficiency during charging/discharging period. $\Delta t$ is the time step which is assumed 1h in this study. Battery state of charge is constrained by its lower and upper limits, i.e.,

$$SOC_{\min} \le SOC(t) \le SOC_{\max} \tag{7}$$

Also there are other constraints that represent the maximum allowable energy taken or added to the battery is limited. This limitation is due to the maximum permissible charging/discharging current to be less than a specified percentage of the battery Ah capacity [23], [24]. This constraint can be written as

$$\left|P_B(t)\right| \le P_b^{\max} \tag{8}$$

Initial $SOC$ is assumed to be $SOC_s$ as stated in following equation:

$$SOC(t)\big|_{t=0} = SOC_S \tag{9}$$

Moreover an additional constraint regarding the battery ending state of charge is considered in this paper that ensures more than a specified percentage of the battery nominal capacity is stored at the end of desired time period. This can be shown as below:

$$SOC(t)\big|_{t=T} \geq SOC_f \tag{10}$$

## 3. Distributed Generation Bids Calculation

DG bids are considered linear, as presented in Equation (11), according to the cost function of the units, if any, the feedback from the market prices and the need to make some profit, necessary for the annual depreciation of the installation cost [25]:

$$B_{gi}(P_{gi}(t)) = b_i.(P_{gi}(t)) + c_i \tag{11}$$

For fuel-consuming units, $c_i$ represents the hourly payback amount for the investment and $b_i$ is their variable cost, i.e., fuel cost. The term $c_i$ also includes startup costs, only when the unit is not in operation or is still in a startup state [4]. Renewable source-based DGs, *e.g.* WT and PV, cannot be regulated and their output is determined by the availability of the primary source, *i.e.* wind or solar irradiance. To account for their production in the optimization functions, WT and PV forecasting is required. To calculate the power output of a WT, two main factors must be known: the wind speed at a certain location and the power curve of the wind turbine. The following is the model used to calculate the output power generated by the wind turbine generator as a function of the wind velocity [26]:

$$P_{WT} = \begin{cases} 0, & V < V_{ci} \\ a.V^2 + b.V + c, & V_{ci} < V < V_{nom} \\ P_{WT,nom} & V > V_{co} \end{cases} \tag{12}$$

where $P_{WT,nom}$, $V_{ci}$, and $V_{co}$ are the rated power, cut-in and cut-out wind speed respectively. Furthermore $V_{nom}$ and $V$ are the rated and actual wind speed. The bid functions of renewable energy sources consider the annual investment cost for depreciation of equipment (AC) (€/kW) and the annual energy production per kW (AP) (kWh/kW) [12].

$$C_{inv} = AC\frac{P_{g\ nom}}{AP} \tag{13}$$

$$AC = \frac{i\ (1+i)^n}{(i+1)^n - 1}.IC \tag{14}$$

where $i$ is the interest rate, $n$ is the depreciation period in years, and IC is the installation cost of the DG.

The power output of the PV module is dependent on the solar irradiance and ambient temperature of the site, as well as the characteristics of the module itself. The following equation can be used to calculate the power output of the PV module, $P_{PV}$ [27]:

$$P_{PV} = P_{STC}\frac{G_{ING}}{G_{STC}}(1 + k(T_c - T_r)) \tag{15}$$

where $P_{STC}$ is photovoltaic module maximum power under standard test conditions (STC) (W), $G_{ING}$ is solar irradiance on the photovoltaic module surface, $G_{STC}$ is irradiance at STC 1000 (W/m$^2$), $k$ is the photovoltaic module temperature coefficient for power (°C$^{-1}$), and $T_c$ and $T_r$ are photovoltaic module temperature and reference temperature (°C), respectively. The details of photovoltaic module temperature calculation can be found in [28].

## 4. Description of the Proposed Optimization Method

Many real-world optimization problems involve simultaneous optimization of several conflicting objectives. A general multiobjective problem can be written as:

$$\min \quad f_i(x) \quad , \quad i = 1,...,N_{obj} \tag{16}$$

$$Subjected\ to: \begin{cases} g_j(x) & j = 1,...,r \\ h_k(x) & k \le 1,...,z \end{cases} \tag{17}$$

where $fi$ is the $i$th objective function, $x$ is a candidate solution and $N_{obj}$ shows the number of goals. Also $r$ and $z$ refer to the number of equality and inequality constraints respectively. The multiobjective optimization with conflicting objectives leads to a set of optimal solutions called non-dominated or Pareto optimal set, instead of one optimal solution [29].

### 4.1. Overview of Shuffled Frog Leaping Algorithm

The shuffled frog leaping algorithm (SFLA) is a meta-heuristic algorithm inspired by the memetic evaluation of a group of frogs, seeking for food [30]. It was originally introduced by Eusuff and Lansey in 2003 [31]. In this algorithm, every member of the population is called a frog. Two local and global strategies are used to generate the new population of frogs and whether modifying the objective function, it is replaced with the existing frogs. Generally, SFLA includes the following three steps.

#### *4.1.1. Generation of the initial population*

The initial population including "$p$" frogs is randomly generated in a way that the position of each frog is in the range of search space. The position of $i$th frog is shown by $Xi=(x1,i,\ x2,i,\ldots,\ xs,i)$, where $s$ is the number of decision variables.

#### *4.1.2. Frogs distribution into Memeplexes*

In this step, the frogs are ordered based on the fitness value. Then, total population is distributed into $m$ memeplex in a way that each memeplex has $n$ frog ($p=m\times n$). The strategy of allocating frogs to memeplexes is in a manner that the first frog is allocated to the first memeplex, the second frog to the second memeplex, and $m$th frog to the $m$th memeplex. Then, $(m+1)$th frog are placed in the first memeplex and this procedure continues until the time of placing all $p$ frogs in $m$ memeplex [32].

#### *4.1.3. Local Search*

In the local search, the worst position of every frog in memeplex is modified according to the position of the best solution of that memeplex or that of all memeplexes. The average of fitness is effective for improving that position. In this regard, the following steps are repeated for each memeplex in the certain iterations:

**Step 1:** The best and worst frogs are determined according to their position value and called $Xb$ and $Xw$, respectively.

**Step 2:** The position of the worst frog ($Xw$) in the memeplex changes according to the position of the best frog ($Xb$), as following:

$$D = rand \times (X_b - X_w) \tag{18}$$

$$X_w^{new} = X_w^{old} + D \tag{19}$$

where $D$ is the vector of frog's mutation and $rand$ is a random number in the range [0, 1]. $X_w^{old}$ and $X_w^{new}$ are the current and new position of the worst frog in the memeplex, respectively. If a better solution is reached in contrast to the previous state, a new frog is replaced with the previous frog and the process leads to the step 5. Otherwise, step 3 is carried out.

**Step 3:** *Xg* is replaced with *Xb* in equation (18) and then the new frog is achieved using equation (19). If an improvement is seen in the solution, the new frog is replaced with the old frog and step 5 is carried out. Otherwise, step 4 is conducted.

**Step 4:** A new frog is randomly generated and replaced with the worst frog of the memeplex.

**Step 5:** The first to fourth steps are repeated in certain numbers.

The distributing process and local search continue until the stopping criterion of the algorithm is estimated. The stopping criterion of the algorithm usually can be chosen based in the stability of the fitness changes of the best solution or the algorithm iteration to a certain number.

4.2. Modified Shuffled Frog leaping Algorithm

Although the SFLA possessed very high velocity, it may face some difficulty in solving the complex models. Therefore, in this paper, the modified shuffled frog leaping algorithm (MSLFA) has been proposed that its searching power has been increased Compared to the standard version. In MSLFA, the movement of the *Xw* in each memeplex has been changed in each iteration of local search. First, the following mutation vector is generated for the worst solution in each iteration:

$$pre\_X_w = X_g + F \times (X_{r1} - X_{r2}) \tag{20}$$

where *Xr1* and *Xr2* are two different frogs that are randomly chosen among the existing frogs in the memeplex. *F* is mutation factor that determines the difference range of *Xr1* and *Xr2,* and *Xg* is the best generated solution until the current iteration. In this regard, the *j*th parameter of $X_w^{new}$ vector in the next iteration is determined by equation (21).

$$X_{wj}^{new} = \begin{cases} pre\_X_{wj} & if \quad rand < CR_g \ \ or \quad j = rm \\ X_{wj}^{old} & otherwise \end{cases} \tag{21}$$

where *rand* is a uniform random number in the range [0, 1], *Crg* is a generic crossing constant in the range [0, 1], and *rm* is a random number that is selected among the range of number of solution parameters and it represents that one of the $X_{wj}^{new}$ parameters among $pre\_x_{wj}$ values.

If the fitness value of new solution is better than the previous solution, the new frog is replaced with the previous one. Otherwise, equations (20) and (21) are repeated by replacing the best solution of each memeplex with *Xg*, and local crossing constant ($CR_b$) with generic crossing constant ($CR_g$). If a better solution does not maintain in this step, a random frog in the search space is generated and replaced with the previous frog. As it is seen, the steps of MSLFA are similar to the classic shuffled frog leaping algorithm (see 4.1.1– 4.1.3). In the proposed method, the difference is that the movement of the worst frog has been modified in the local search to improve the efficiency of the SFLA. In this regard, equations (18) and (19) are replaced with equations (20) and (21). Fig. 1 depicts the MSLFA procedure step by step.

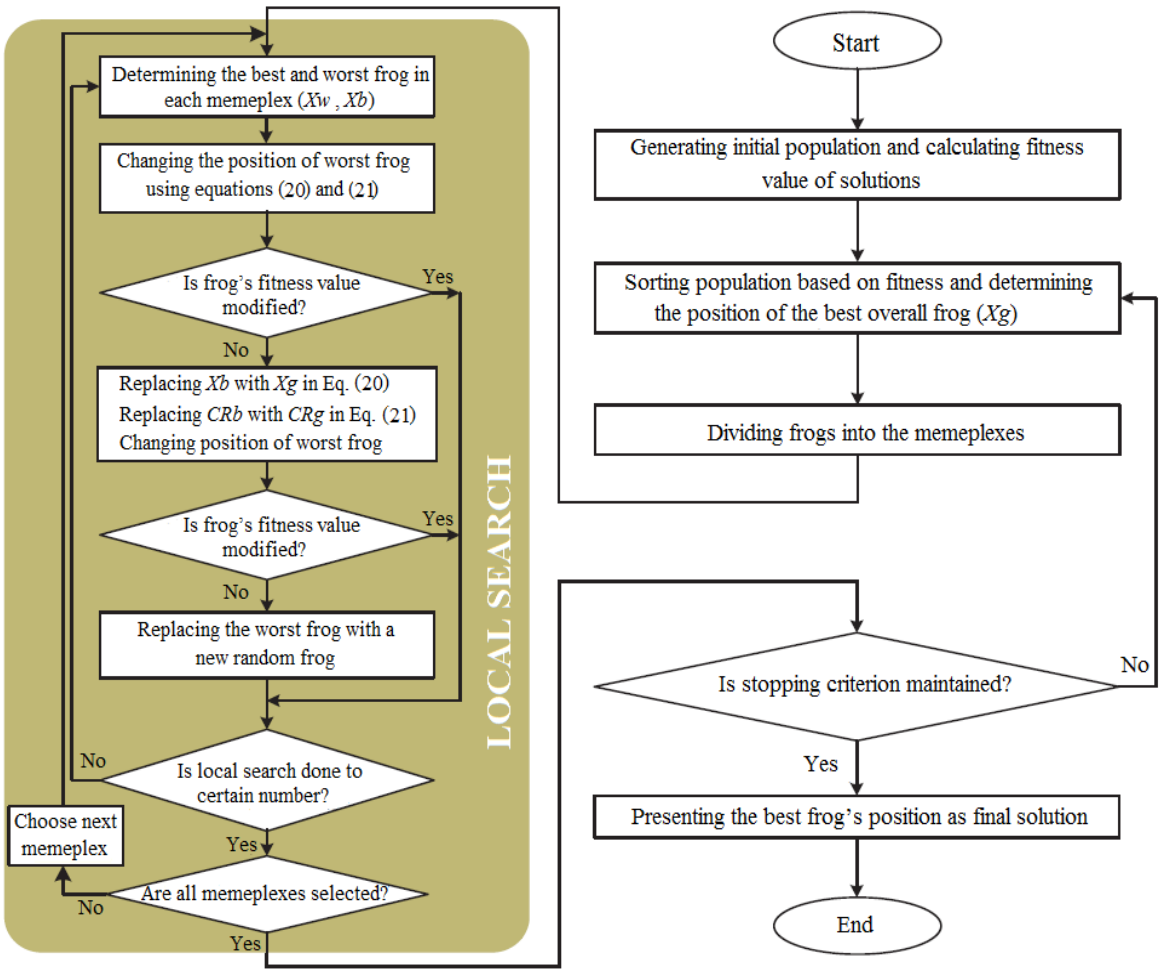


**Fig. 1.** Proposed MSLFA Flowchart.

4.3. Application of MSFLA to Solve the EEOM Problem

Fig. 1 shows flowchart of the proposed optimization method. The details of utilization of MSFLA to solve the EEOM problem are explicated in the following.

**Frogs Structure and Initialization:** In the process of initialization, the position of set of frogs is randomly generated. In this paper, the position of each of frogs is a solution for EEOM problem. Therefore, the position of *j*th frog is shown as a vector of *Xj*. In the process of initialization, the position of each frog should be chosen in a manner that equal and unequal constraints are maintained.

**Calculation of Frogs Fitness:** The extent of corresponding objective function (Eqs. (1) and (2)) for each frog has to be calculated in order to determine the fitness for each of frogs.

**Sorting and Distribution of Frogs into the Memeplex:** Frogs are sorted based on their fitness value and distributed based on the strategy proposed in 4.1.2.

**Local Search:** For each of memeplexes, local search is conducted based on the procedure proposed in 4.1.3 and based on the modified strategy explicated in 4.2.

**Maintain Unequal Constraints:** There is a possibility that the constraints of the EEOM problem (Eq. (4)) have been violated when generating a new position for the worst frogs in the process of local search. In this paper, in order to maintain the unequal constraint, the wall absorption rule [33] has been used.

**Stopping Criterion:** The stopping criterion of algorithm has been set as the maximum qualified iteration in a way that the searching process is carried out for a certain number of iteration and finally the position of best frog is the final solution for EEOM problem.

## 5. Case Study

A typical low voltage (LV) grid-connected MG comprising variety of DGs, storage device and consumers is shown in Fig. 2. The MG is supplied from the utility (MV distribution grid) through an MV/LV transformer [12]. The MG comprises three feeders: one serving a primarily residential area, one industrial feeder serving a small workshop, and one feeder with commercial consumers. A variety of DG sources, such as a MT, a proton-exchange membrane fuel cell (PEM-FC), a directly coupled WT, and several PVs are installed in the residential feeder. It is assumed that all DG sources produce active power at unity power factor, i.e., neither requesting nor producing reactive power. The MGCC is located downstream of the transformer and the micro-source controllers (MCs) are installed close to the DGs. The MGCC optimizes the MG operation according to the open market prices, bids received by the DG sources and forecast loads, and sends signals to the MCs of DG sources to be committed, and if applicable, to determine the level of their production.

It should be noted that, the optimization procedure depends on the market policy adopted in the MG operation. Accordingly, minimum and maximum operating limits of the DG sources and related bid coefficients are given in Table 1, and hourly energy price data are given in Table 2 [4]. The detail of MG's load curve and typical 24-hour emission curve of the upstream network can be found in [2]. Normalized data of actual wind power and PV production during the day is provided in Fig. 3. Moreover we equipped the case study with a battery bank of size 40kWh, where $SOC_{min}$ and $SOC_{max}$ are set to 16kWh and 40kWh respectively and maximum charging and discharging capability of the battery bank is constrained by 4kW in each time step.

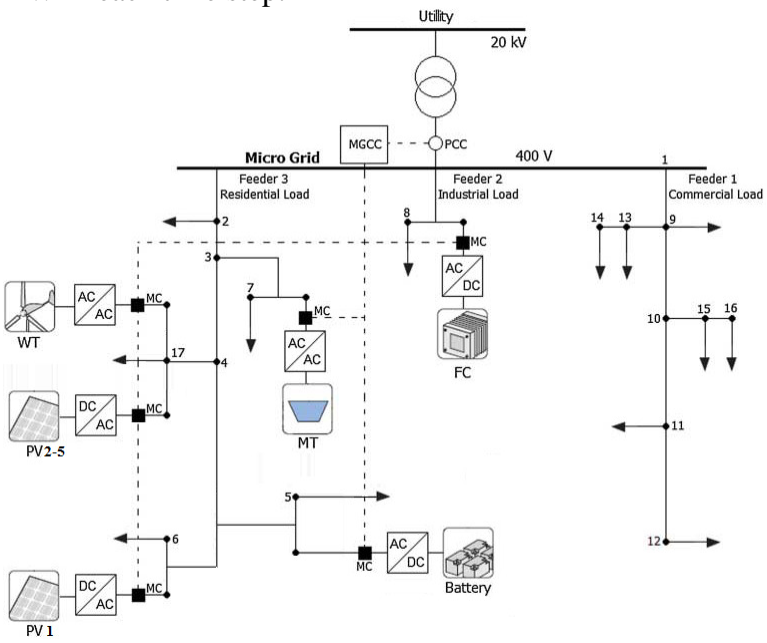


**Fig.2.** A typical low voltage MG comprises a variety of DGs.

**Table 1.** Installed DGs in MG.

| DG Type | Pmin (KW) | Pmax (KW) | bi (€ct/KWh) | ci (€ct/h) | CO2 (g/KWh) |
|---|---|---|---|---|---|
| MT | 6 | 30 | 4.370 | 85.060 | 724.6 |
| FC | 3 | 30 | 2.840 | 255.18 | 489.4 |
| WT | 0 | 15 | 10.63 | 0 | 0 |
| PV1 | 0 | 3 | 54.84 | 0 | 0 |
| PV2 | 0 | 2.5 | 54.84 | 0 | 0 |
| PV3 | 0 | 2.5 | 54.84 | 0 | 0 |
| PV4 | 0 | 2.5 | 54.84 | 0 | 0 |
| PV5 | 0 | 2.5 | 54.84 | 0 | 0 |

**Table 2.** Hourly energy prices.

| Hour | Price (€/MWh) | Hour | Price (€/MWh) | Hour | Price (€/MWh) | Hour | Price (€/MWh) |
|---|---|---|---|---|---|---|---|
| 1 | 22.640 | 7 | 23.010 | 13 | 149.86 | 19 | 35.160 |
| 2 | 19.000 | 8 | 38.370 | 14 | 40.000 | 20 | 43.950 |
| 3 | 13.980 | 9 | 149.86 | 15 | 201.00 | 21 | 117.12 |
| 4 | 12.000 | 10 | 40.000 | 16 | 194.99 | 22 | 54.000 |
| 5 | 11.530 | 11 | 40.000 | 17 | 60.000 | 23 | 30.000 |
| 6 | 19.940 | 12 | 40.000 | 18 | 41.300 | 24 | 25.570 |

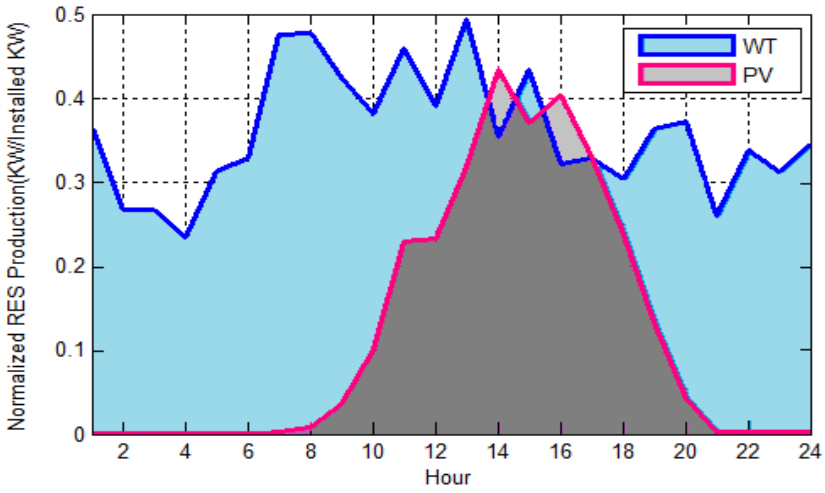


**Fig. 3.** Normalized RES hourly production (KW/ Installed KW).

## 6. Simulation Results

In the EEOM problem, decision variables involve DG units' production, energy to be requested from the main distribution grid and the amount of charging or discharging of storage devices during the specified period which should be effectively determined in order to achieve desired performance. In this regard, the simulations were carried out starting from a base case (named case A) in which all system demand has to be supplied by the upstream network and neither DGs nor storage devices exist. Under these assumptions, an operating cost of €469.76 resulted while the total emission is 2650kg. To evaluate the influence of aggregating DGs and storage devices under the coordination of a central MG management system, three sets of simulations are considered and compared with case A.

The proposed MSFLA-based approach was implemented in MATLAB Version 2013a and run on a 2.60 GHz PC with 4.0GB RAM. Thirty consecutive test runs were performed for each case examined. Parameters of MSFLA-based approach, are given in Table 3.

### 6.1. Economic Operation Management of MG (Case1)

In this case, it is assumed that MGCC aims for optimal DG sources production, storage devices utilization and the amount of energy to be requested from the utility in order to meet system demand in the most economical way. The best results obtained using the proposed MSFLA for case 1 are shown in Tables 4. By analyzing these results, it can be seen that all equality and inequality constraints are satisfied.

**Table 3.** Best parameters for MSFLA implementation.

| Population Size | Number of iterations | Local search iterations | Number of memeplexes | CRg | CRb | F |
|---|---|---|---|---|---|---|
| 300 | 150 | 10 | 10 | 0.85 | 0.3 | 0.8 |

**Table 4.** Best solutions obtained for the MG operation management problem using MSFLA for case 1.

| Time (h) | Load (KW) | Active Power (KW) | | | | | | SOC (KWh) | Cost (€ct/h) | Emission (kg) |
|---|---|---|---|---|---|---|---|---|---|---|
| | | PV | WT | MT | FC | Battery | Utility | | | |
| 1 | 68 | 0 | 0 | 6 | 3 | +3.535 | 55.465 | 23.515 | 5.0055 | 46.028 |
| 2 | 60 | 0 | 0 | 6 | 3 | +4.000 | 47.000 | 27.491 | 4.6428 | 38.716 |
| 3 | 55 | 0 | 0 | 6 | 3 | +4.000 | 42.000 | 31.464 | 4.3370 | 33.116 |
| 4 | 52 | 0 | 0 | 6 | 3 | +4.000 | 39.000 | 35.433 | 4.2178 | 31.166 |
| 5 | 49 | 0 | 0 | 6 | 3 | +4.000 | 36.000 | 39.397 | 4.1649 | 29.216 |
| 6 | 51 | 0 | 0 | 6 | 3 | +0.643 | 41.358 | 40.000 | 4.5745 | 32.698 |
| 7 | 80 | 0 | 0 | 6 | 3 | +0.040 | 70.960 | 40.000 | 5.3826 | 51.940 |
| 8 | 100 | 0 | 0 | 6 | 30 | +0.040 | 63.960 | 40.000 | 6.9707 | 63.802 |
| 9 | 130 | 0 | 6.360 | 30 | 30 | –1.670 | 65.310 | 38.290 | 15.528 | 82.898 |
| 10 | 150 | 0 | 5.715 | 30 | 30 | –4.000 | 88.285 | 34.252 | 38.287 | 104.66 |
| 11 | 170 | 0 | 6.885 | 30 | 30 | –4.000 | 107.11 | 30.218 | 45.943 | 120.67 |
| 12 | 180 | 0 | 5.850 | 30 | 30 | –4.000 | 118.15 | 26.188 | 50.247 | 130.05 |
| 13 | 180 | 0 | 7.410 | 30 | 30 | +1.896 | 110.69 | 28.057 | 22.942 | 136.04 |
| 14 | 180 | 0 | 5.325 | 30 | 30 | –4.000 | 118.68 | 24.029 | 50.401 | 136.03 |
| 15 | 180 | 0 | 6.495 | 30 | 30 | –4.000 | 117.50 | 20.005 | 28.266 | 118.55 |
| 16 | 175 | 0 | 4.815 | 30 | 30 | –3.985 | 114.17 | 16.000 | 26.785 | 105.45 |
| 17 | 170 | 0 | 0 | 30 | 30 | +0.016 | 109.98 | 16.000 | 12.164 | 107.91 |
| 18 | 180 | 0 | 0 | 6 | 30 | +1.421 | 142.58 | 17.405 | 10.405 | 125.96 |
| 19 | 200 | 0 | 0 | 6 | 30 | +4.000 | 160.00 | 21.387 | 10.142 | 203.03 |
| 20 | 190 | 0 | 0 | 30 | 30 | +2.678 | 127.32 | 24.044 | 11.161 | 182.84 |
| 21 | 180 | 0 | 3.901 | 30 | 30 | –4.000 | 120.10 | 20.020 | 19.109 | 159.73 |
| 22 | 160 | 0 | 0 | 30 | 30 | –4.000 | 104.00 | 16.000 | 10.749 | 113.22 |
| 23 | 140 | 0 | 0 | 6 | 30 | +0.016 | 103.98 | 16.000 | 7.6361 | 97.018 |
| 24 | 100 | 0 | 0 | 6 | 3 | +0.016 | 90.984 | 16.000 | 6.0763 | 74.054 |
| **Total Cost (€ct) & Total Emission (kg)** | | | | | | | | | **405.14** | **2324.8** |

As shown in Table 4, the total operation cost of the MG decreases in comparison with the base case and demonstrates a reduction of %13.8 (% 12.27) in related cost ($CO_2$). As shown in Tables 4, the output power of PV has minimum value throughout the day, because PV and WT have much higher bids than the other DGs. Also, the output powers of FC and MT have minimum value during periods of the day with low values of the market prices and maximum values during periods with high market prices. The battery charging process corresponds with periods of low market prices and in the periods that the market prices are substantially high, we can benefit from supplying loads by discharging the battery bank. It is noticeable that during hours with lower market prices, the active power is exchanged from the utility to the MG. For example during h=10 when 150kWh is demanded by local loads, 61.715KWh is supplied by local DGs and battery delivers 4kWh (-4kWh), the remainder energy (88.285kWh) is requested from the main grid to cover all demand.

6.2. Environmental Operation Management of MG (Case2)

In this case, the strategy is desired by MGCC for optimal DG sources production, storage devices utilization and the amount of energy to be requested from the utility in order to supply the local loads with the lowest emission level. It should be noted that in comparison with case 1, consumers are supplied with greener electricity in expense of more operating cost. Also according to the daily scheduling depicted in Table 5, in this case MG is more focused on local production so that the algorithm has set the output power of RESs (PV and WT) to their maximum available power. The output power of FC has maximum value throughout the day and the output power of MT is increased in the periods that the

emitted pollutants of upstream network are high. For example from h=9–15 and h=18–24 the output power of MT set to maximum value. It is also noticeable that batteries have been charged during hours with lower emission levels in order to improve grid's performance by providing their stored energy during hours with high emission levels. In this case, total operation cost is €430.84 whereas 2219.6 kg $CO_2$ is produced which demonstrates %8.3 and %16.24 reduction respectively in comparison with the base case.

**Table 5.** Best solutions obtained for the MG operation management problem using MSFLA for case 2.

| Time (h) | Load (KW) | Active Power (KW) | | | | | | SOC (KWh) | Cost (€ct/h) | Emission (kg) |
|---|---|---|---|---|---|---|---|---|---|---|
| | | PV | WT | MT | FC | Battery | Utility | | | |
| 1 | 68 | 0 | 5.460 | 30 | 30 | –3.980 | 6.5201 | 16.000 | 6.1132 | 35.376 |
| 2 | 60 | 0 | 4.005 | 6 | 30 | +3.937 | 16.062 | 19.921 | 5.3970 | 35.782 |
| 3 | 55 | 0 | 4.005 | 6 | 30 | +4.000 | 10.996 | 23.901 | 5.2079 | 31.376 |
| 4 | 52 | 0 | 3.510 | 6 | 30 | +4.000 | 8.4898 | 27.877 | 5.0876 | 29.748 |
| 5 | 49 | 0 | 4.680 | 6 | 30 | +4.000 | 4.3201 | 31.849 | 5.1561 | 27.038 |
| 6 | 51 | 0 | 4.935 | 6 | 30 | +4.000 | 6.0649 | 35.818 | 5.3216 | 28.172 |
| 7 | 80 | 0.026 | 7.140 | 6 | 30 | +4.000 | 32.834 | 39.782 | 6.2294 | 45.572 |
| 8 | 100 | 0.104 | 7.155 | 6 | 30 | +0.258 | 56.483 | 40.000 | 7.5213 | 58.929 |
| 9 | 130 | 0.455 | 6.360 | 30 | 30 | +0.040 | 63.153 | 40.000 | 15.967 | 83.839 |
| 10 | 150 | 1.298 | 5.715 | 30 | 30 | –4.000 | 86.998 | 35.960 | 38.483 | 103.56 |
| 11 | 170 | 2.990 | 6.885 | 30 | 30 | –4.000 | 104.13 | 31.924 | 45.388 | 118.13 |
| 12 | 180 | 3.027 | 5.849 | 30 | 30 | –4.000 | 115.13 | 27.892 | 49.650 | 127.48 |
| 13 | 180 | 4.134 | 7.410 | 30 | 30 | –4.000 | 112.47 | 23.864 | 24.275 | 130.43 |
| 14 | 180 | 5.629 | 5.319 | 30 | 30 | –4.000 | 113.12 | 19.840 | 50.264 | 130.99 |
| 15 | 180 | 4.810 | 6.495 | 30 | 30 | +3.979 | 104.73 | 23.799 | 31.542 | 120.93 |
| 16 | 175 | 5.239 | 4.815 | 6 | 30 | +4.000 | 124.95 | 27.775 | 33.325 | 105.44 |
| 17 | 170 | 4.290 | 4.935 | 6 | 30 | +4.000 | 120.78 | 31.747 | 15.120 | 102.73 |
| 18 | 180 | 3.094 | 4.545 | 30 | 30 | +0.381 | 112.02 | 32.096 | 12.401 | 120.98 |
| 19 | 200 | 1.728 | 5.460 | 30 | 30 | –4.000 | 136.82 | 28.064 | 11.523 | 184.56 |
| 20 | 190 | 0.558 | 5.545 | 30 | 30 | –4.000 | 127.85 | 24.036 | 11.633 | 174.25 |
| 21 | 180 | 0.039 | 3.900 | 30 | 30 | –4.000 | 120.06 | 20.012 | 19.101 | 159.69 |
| 22 | 160 | 0 | 5.070 | 30 | 30 | –3.995 | 98.922 | 16.000 | 11.015 | 109.17 |
| 23 | 140 | 0 | 4.680 | 30 | 30 | +0.016 | 75.304 | 16.000 | 8.3230 | 92.922 |
| 24 | 100 | 0 | 5.190 | 30 | 30 | +0.016 | 34.794 | 16.000 | 7.0076 | 62.540 |
| **Total Cost (€ct) & Total Emission (kg)** | | | | | | | | | **430.84** | **2219.6** |

Under the same system data, control variable limits and constraints, the results obtained using the proposed MSFLA method reported in this article are compared to some other well-known algorithms such as GA, CQGA [20], DE [19], CDE [3], PSO [12] and SFLA [35] in Table 6. As shown in Table 6, the proposed MSFLA outperforms many techniques used to solve EEOM problem, because the results obtained using MSFLA are either better than or comparable to those obtained using other techniques. The calculated standard deviation of MSFLA is very low, which confirms the excellent robustness of the proposed MSFLA.

Note that, the standard deviation for cases 1 and 2 is calculated based on total operation cost and emission level, respectively. Figures 4(a) and 4(b) illustrate the convergence characteristics of Mentioned methods in case 1 and 2, respectively. In these figures, the best results of 30 run characteristics are depicted for 150 iterations for above mentioned methods. As seen in Figure 4, the MSFLA shows better performance than the other methods in success rate and solution quality.

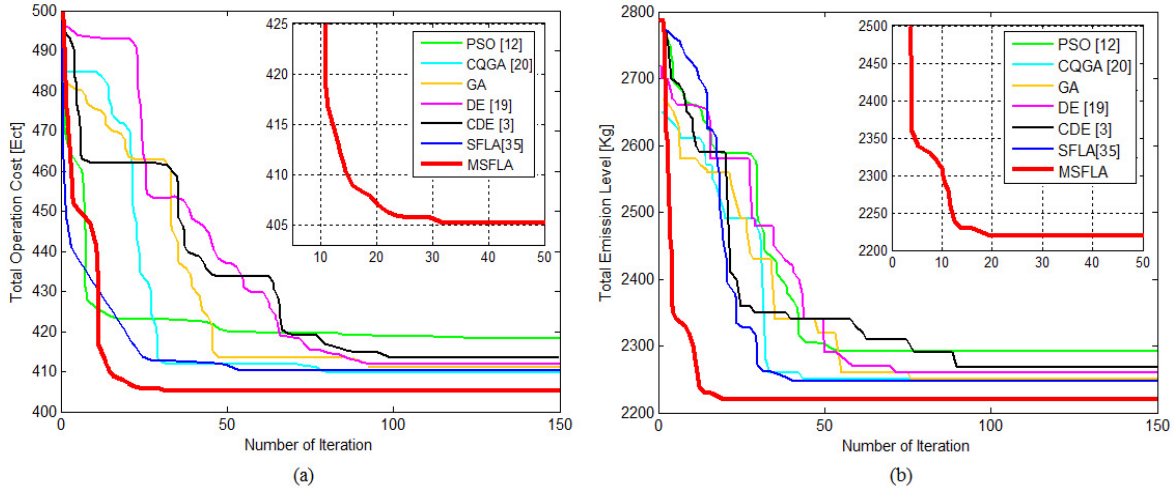


**Fig. 4.** Convergence characteristics of different methods for case 1 (a) and case 2 (b).

**Table 6.** Comparison of the numerical results obtained using the different methods for cases 1 and 2.

| Case No. | Method | Best cost (€) | Best emission level (Kg) | Worst cost (€) | Worst emission level (Kg) | Standard deviation |
|---|---|---|---|---|---|---|
| Case 1 | GA | 411.13 | 2419.11 | 433.83 | 2447.19 | 6.30987 |
| | DE [19] | 412.07 | 2397.49 | 439.08 | 2425.08 | 7.60698 |
| | CQGA [20] | 409.74 | 2407.22 | 429.52 | 2473.00 | 3.32089 |
| | DE-PSO [34] | 410.77 | 2385.41 | 422.19 | 2391.09 | 3.14374 |
| | CDE [3] | 413.36 | 2370.65 | 437.43 | 2411.24 | 6.80944 |
| | SFLA [35] | 410.19 | 2412.30 | 426.84 | 2493.14 | 3.17905 |
| | PSO [12] | 418.37 | 2371.63 | 419.82 | 2389.30 | 0.00821 |
| | **MSFLA** | **405.14** | **2324.80** | **405.16** | **2325.90** | **0.00029** |
| Case 2 | GA | 448.32 | 2252.42 | 453.66 | 2379.12 | 36.2829 |
| | DE [19] | 445.38 | 2257.02 | 450.63 | 2405.87 | 42.7765 |
| | CQGA [20] | 446.11 | 2244.80 | 458.19 | 2357.66 | 32.2693 |
| | DE-PSO [34] | 440.19 | 2249.34 | 443.55 | 2331.73 | 20.8147 |
| | CDE [3] | 442.07 | 2264.63 | 456.47 | 2363.69 | 27.9386 |
| | SFLA [35] | 447.11 | 2247.27 | 462.91 | 2340.72 | 25.2638 |
| | PSO [12] | 439.52 | 2292.09 | 450.28 | 2303.04 | 3.11074 |
| | **MSFLA** | 430.84 | 2219.60 | 430.91 | 2221.01 | **0.21695** |

**Note:** GA = genetic algorithm; CQGA= chaotic quantum genetic algorithm; PSO = particle swarm optimization; DE = differential evolution; CDE = Chaotic differential evolution; SFLA = shuffled frog leaping algorithm; MSFLA = modified shuffled frog leaping algorithm.

### 6.3. Environmental/Economic Operation Management of MG (Case3)

In the previous cases, MG operation has been optimized in two extreme conditions, i.e., achieving the minimum operation cost or minimum environmental impact. In this case the EEOM problem is handled as a multiobjective optimization problem where both cost and emission are optimized simultaneously. Among most common multiobjective optimization approaches, a frequently used method is to combine all objectives to form a single function. In this method every objective according to its relative importance is weighted using a coefficient. The coefficients could be fixed at the beginning of optimization process or altered continuously in a range to reach the entire Pareto optimal set of solutions. It should be noted that in the former approach the preferences of the decision maker or relative importance of different goals must be specified in advance and in latter one in order to generate for instance 50 non-dominated solutions, it is required to apply the algorithm 50 times separately [34].

However in a dynamic situation with lack of preference information, the desired strategy has to be selected from a pool of provided efficient solutions which have been

obtained through an effective mechanism. So to facilitate the process of decision making, MGCC should be provided with the true Pareto front in order to increase the reliability of the decisions that have to be made [36]. Applying the proposed MSFLA on the EEOM problem in order to minimize operation cost and emission simultaneously, 87 non-dominated solutions that well cover the entire Pareto front of the problem have been obtained in a single run.

The minimum operation cost, the minimum emission level, and number of optimal solution obtained by using different methods for case 3 are listed in Table 7. Also, optimal Pareto fronts obtained from MSFLA is depicted in Fig. 5 and Compared to other methods. In the optimal Pareto front obtained from MSFLA, the point marked "a" (€406.83) is the best choice if the only goal is to minimize operation costs and point marked "b" (2220.39kg) is best to minimize emissions, regardless of operation costs.

From Fig. 5, it can be seen that the MSFLA shows better performance than the other methods in success rate and solution quality. Also, the proposed MSFLA preserves the diversity of non-dominated solutions over the trade-off surface so that the MGCC can choose a suitable strategy based on desired preferences.

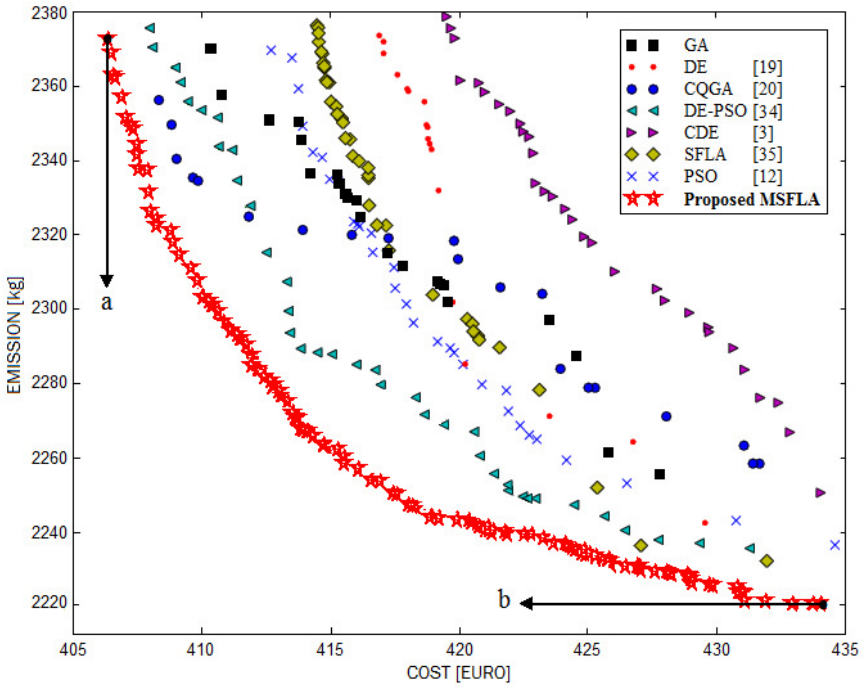


**Fig.5.** Optimal Pareto front obtained using different methods for case 3.

**Table 7.** Comparison of the numerical results obtained using the different methods for case 3.

| Method | Number of non-dominated solutions | Minimum cost (€) | Minimum emission level (Kg) |
|---|---|---|---|
| GA | 22 | 410.38 | 2258.14 |
| DE [19] | 18 | 417.82 | 2246.13 |
| CQGA [20] | 20 | 409.06 | 2263.92 |
| DE-PSO [34] | 38 | 408.67 | 2237.55 |
| CDE [3] | 31 | 421.23 | 2254.77 |
| SFLA [35] | 36 | 114.78 | 2233.89 |
| PSO [12] | 30 | 413.91 | 2238.46 |
| **Proposed MSFLA** | **87** | **406.83** | **2220.39** |

## 7. Conclusion

In this paper proposed a new method based on multiobjective modified shuffled frog leaping algorithm to solve the MG environmental/economic operation management problem properly. In this regard, The proposed MSFLA includes a new way of frog distribution into memeplexes and a new frog leaping rule to improve the local exploration and performance of the SFLA. The EEOM problem has been formulated in multiobjective optimization framework with competing total operation cost and total emission goals in a highly constrained environment. The proposed method has been tested and investigated in a typical grid-connected MG consisting of FC, WT, PV, MT and Battery energy storage devices. The simulation results show the efficiency of the proposed method to solve both environmental and economical operation management problems under Separate operational scenarios of the MG. Moreover, the results obtained using the MSFLA are either better than or comparable to those obtained using well-known methods reported in the literature. Also, the proposed method is efficient for solving the single objective and multiobjective optimization problem of MG and providing multiple Pareto optimal solutions in a single run, that well cover the entire Pareto front and preserves the diversity of non-dominated solutions over the trade-off surface. In addition it can be seen that aggregating multiple individual DGs and storage devices under the control of a central management unit, provides more opportunity and flexibility in utilizing available resources according to desired preferences. Furthermore it has been shown that an intelligent schedule to charge and discharge storage devices can lead to considerable reduction in cost and environmental impacts.

## References

[1] IEEE Standard 1547.4-2011, “IEEE Guide for Design, Operation, and Integration of Distributed Resource Island Systems with Electric power systems”, 2011.

[2] N. D. Hatziargyriou, A. G. Anastasiadis, J. Vasiljevska, A. G. Tsikalakis, “Quantification of Economic, Environmental and Operational Benefits of Microgrids” IEEE Bucharest Power Tec. Conference, Bucharest, Romania, 2009.

[3] M. Hemmati, N. Amjady, M. Ehsan, "System Modeling and Optimization for Islanded Micro-Grid Using Multi- Cross Learning-Based Chaotic differential evolution algorithm", International Journal of Electrical Power & Energy Systems, Vol. 56, pp. 349-360, 2014.

[4] A. G. Tsikalakis, N. D. Hatziargyriou, “Centralized Control for Optimizing Microgrids Operation”, IEEE Transactions on Energy Conversion, Vol. 23, No. 1, pp. 241-248, 2008.

[5] S. Chakraborty, M. D.Weiss, and M. G. Simoes, “Distributed Intelligent Energy Management System for a Single-Phase High-Frequency AC Microgrid”, IEEE Transactions on Industrial Electronics, Vol. 54, No. 1, pp. 97–109, 2007.

[6] C. Chen, S. Duan, T. Cai, B. Liu, and G. Hu, “Smart Energy Management System for Optimal Microgrid Economic Operation”, IET Renewable Power Generation, Vol. 5, No. 3, pp. 258–267, 2011.

[7] A. A. Moghaddam, A. Seifi, T. Niknam, and M. R. A. Pahlavani, “Multi-objective Operation Management of a Renewable MG (Micro-grid) with Back-up Micro-turbine/Fuel Cell/Battery Hybrid Power Source”, international journal of Energy, Vol. 36, No. 11, pp. 6490–6507, 2011.

[8] H. Wu, X. Liu, and M. Ding, “Dynamic Economic Dispatch of a Microgrid: Mathematical Models and Solution Algorithm”, International Journal of Electrical Power and Energy Systems, Vol. 63, No. 1, PP. 336–346, 2014.

[9] B. Tomoiaga, M. D. Chindric, A. Sumper, and M. Marzband, "The Optimization of Microgrids Operation Through a Heuristic Energy Management Algorithm", Advanced Engineering Forum, Vol. 8–9, pp. 185–194, 2013.

[10] S. Chakraborty, M. D. Weiss and M. G. Simoes, "Distributed Intelligent Energy Management System for a Single- Phase High Frequency AC Microgrid," IEEE Transactions on Industrial Electronics, Vol. 54, No. 1, pp. 97-109, 2007.

[11] A. Dukpa, I. Dugga, B. Venkatesh and L. Chang, "Optimal Participation and Risk Mitigation of Wind Generators in an Electricity Market," IET Renewable Power Generation, Vol. 4, No. 2, pp. 165-175, 2010.

[12] J. Radosavljev, M. Jevti, D. Klimenta, "Energy and operation management of a microgrid using particle swarm optimization", Engineering Optimization, Vol. 47, No. 6, pp. 1-20, 2015.

[13] H. Morais, P. Kádár, P. Faria, Z. A. Vale and H. M. Khodr, "Optimal Scheduling of a Renewable Microgrid in an Isolated Load Area Using Mixed-Integer Linear Programming", Renewable Energy, Vol. 35, No. 1, pp. 151-156, 2010.

[14] O. Hafez and K. Bhattacharya, "Optimal Planning and Design of a Renewable Energy Based Supply System for Microgrids", Renewable Energy, Vol. 45, No. 1, pp. 7-15, 2012.

[15] S. Mizani, A. Yazdani, "Optimal design and operation of a grid-connected Microgrid", IEEE Electrical Power & Energy Conference (EPEC), pp. 1–6, Montreal, 2009.

[16] W. Cheng-Shan, Y. Bo, X. Jun, G. Li, "Multi-scenario, multiobjective optimization of grid-parallel Microgrid", 4th International Conference on Electric Utility Deregulation and Restructuring and Power Technologies (DRPT), pp. 1638–1646, July 2011.

[17] F. A. Mohamed, and H. N. Koivo, "System Modeling and Online Optimal Management of Microgrid using Mesh Adaptive Direct Search", International Journal of Electrical Power and Energy Systems, Vol. 32, No. 5, pp. 398–407, 2010.

[18] F. A. Mohamed, H. N. Koivo, "Multiobjective optimization using Mesh Adaptive Direct Search for power dispatch problem of Microgrid" International Journal of Electrical Power & Energy Systems, Vol. 42, No. 1, pp.728–735, 2012.

[19] H. Vahedi, R. Noroozian, S. H. Hosseini, "Optimal management of Microgrid using differential evolution approach", 7th International Conference on European Energy Market (EEM), pp. 1–6, Madrid, June 2010.

[20] G. Liao, "Solve environmental economic dispatch of Smart Microgrid containing distributed generation system using chaotic quantum genetic algorithm", International Journal of Electrical Power & Energy Systems, Vol. 43, No. 1, pp.779–787, 2012.

[21] Y. Zhang, N. Gatsis, and G. B. Giannakis, "Robust Energy Management for Microgrids with High-Penetration Renewables", IEEE Transactions on Sustainable Energy, Vol. 4, No. 4, pp. 944–953, 2013.

[22] F. A. Mohamed, H. N. Koivo, "Online Management of Microgrid with Battery Storage Using Multiobjective Optimization", international conference on power engineering, energy and electrical drives, pp. 231-236, 2007.

[23] R. Chedid, S. Rahman, "Unit Sizing And Control of Hybrid Wind-Solar Power Systems", IEEE Transactions On Energy Conversion, Vol. 12, No. 1, pp. 2977-2988, March 1997.

[24] M. Pipattanasomporn, "A Study of Remote Area Internet Access with Embedded Power Generation", PhD dissertation, Virginia Polytechnic Institute and State University, Virginia, Dec. 2004.

[25] N. D. Hatziargyriou, A. G. Anastasiadis, A. G. Tsikalakis, and J. Vasiljevska, "Quantification of Economic, Environmental and Operational Benefits due to Significant Penetration of Microgrids in a Typical LV and MV Greek Network", European Transaction on Electrical Power, Vol. 21, No. 2, pp. 1217–1237, 2011.

[26] R. Chedid, H. Akiki, and S. Rahman, "A Decision Support Technique For The Design Of Hybrid Solar-Wind Power Systems", IEEE Transaction on Energy Conversion, Vol. 13, No. 1, pp.76-83, 1998.

[27] Y. M. Atwa, E. F. El-Saadany, M. M. A. Salama, R. Seethapathy, M. Assam, and S. Counti, "Adequacy Evaluation of Distribution System Including Wind/Solar DG During Different Modes of Operation", IEEE Transactions on Power Systems, Vol. 26, No. 4, pp. 1945–1952, 2011.

[28] J. Oh, "Building Applied and Back Insulated Photovoltaic Modules: Thermal Models", Master thesis, Arizona State University, 2010.

[29] M. A. Abido, "Environmental/economic power dispatch using multiobjective evolutionary algorithms", IEEE Transaction on Power Systems, Vol. 18, No. 4, pp. 1529–1537, Nov. 2003.

[30] M. M. Eusuff, K. Lansey, F. Pasha, "Shuffled frog leaping algorithm: a memetic meta-heuristic for discrete optimization", Journal of Engineering Optimization, Vol. 38, No. 2, pp.129–54, 2006.

[31] M. M. Eusuff, K. Lansey, "Optimization of water distribution network design using the frog leaping algorithm", Journal of Water Resources Planning and Management, Vol. 129, No. 3, pp.5–21, 2003.

[32] M. Jadidoleslam, A. Ebrahimi, "Reliability constrained generation expansion planning by a modified shuffled frog leaping algorithm", Electrical Power and Energy Systems, Vol. 64, pp. 743–751, 2015.

[33] J. Robinson, R. Samii, "Particle Swarm Optimization in Electromagnetic", IEEE Transaction on Power Systems, Vol. 52, No. 2, pp. 397–407, 2004

[34] N. Bazmohammadi, A. Karimpour, S. Bazmohammadi, "Optimal operation management of a microgrid based on MOPSO and Differential Evolution algorithms," 2nd Iranian Conference on Smart Grids (ICSG), 2012.

[35] A. Jalilvand, "Optimal Management of Micro-grid in Island-Mode Using Shuffled Frog-Leaping Algorithm", International Review of Electrical Engineering, Vol. 6, No. 5, pp. 2410-2410, 2011.

[36] S. Agrawal, Y. Dashora, M. K. Tiwari, Y. J. Son, "Interactive Particle Swarm: A Pareto-Adaptive Metaheuristic to Multiobjective Optimization", IEEE Transaction on Systems, Man, and Cybernetics—Part A: Systems and Humans, Vol. 38, No. 2, pp. 258–277, March. 2008.